Electromagnetic Beam Position Monitoring Model for Particle Energy Linear Accelerator

Sabir Hussain, Alistair Duffy, Hugh Sasse

School of Engineering and Sustainable Development, Faculty of Technology, De Montfort University
Gateway Leicester UK
shussain95@yahoo.co.uk, apd@dmu.ac.uk, hgs@dmu.ac.uk

***Abstract* —** Beam Position Monitoring (BPM) systems are crucial in particle acceleration facilities such as linear and circular accelerators. They are used to maintain a stable and precise beam position to achieve a high level of beam quality. BPMs are also essential for accelerator commissioning, performance optimisation, and fault analysis. Beam functional properties information, such as displacement from the desired axis, information about synchrotron oscillations and betatron movements can be derived from data gathered in BPM systems. Medical linear accelerators (linacs) also employ BPM measurements to ensure optimal generation of treatment radiation. The most common form of analysis is to use a multi-physics based approach and model the beam as a stream of electrons, often involving Monte Carlo implementation – an accurate but computationally expensive approach. This paper presents a simple, but robust and efficient, CST microwave model of the linear accelerator (linac) beam, generated using a simplified approach to beam modeling that uses a conducting filament in place of the particle. This approach is validated by comparison with published work. An approach to BPM using the method applied in this paper opens up opportunities to further analyze the overall design and that of components of particle accelerator systems using commonly available full-wave electromagnetic simulators without the need to include specific particle solutions.

***Index terms* –** Beam position monitoring, BPM electromagnetic**,** linear accelerators, particle accelerators, pickup electrode.

I. INTRODUCTION

A. Linear accelerators

A Linear accelerator (linac) is a device that accelerates electrons to high energies through a waveguide [1]. Fig. 1 represents an overview of the structure of a medical linear accelerator, typically up to 22 MeV which is the sufficient energy for practical radiotherapy.

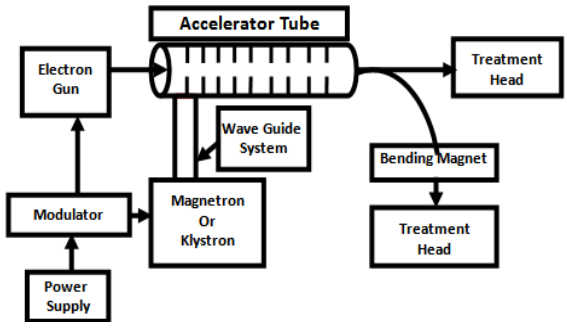

Fig. 1. A block diagram of medical linear accelerator [2].

The big challenge to the application of a linac is the production of a monoenergetic high current electron beam of a small focal spot, ensuring a production of sharply focused X-rays [2]. There are two main classes of accelerators: electrostatic and cyclic. The following discussion concentrates on the cyclic type of accelerator, which is widely used in radiotherapy. The electric fields used in cyclic accelerators are variable and non-conservative, associated with a variable magnetic field, resulting in some closed paths along which the kinetic energy gained by the particle differs from zero. If the particle is made to follow such a closed path

many times, a process of gradual acceleration is obtained that is not limited to the maximum voltage drop existing in the accelerator. Thus, the final kinetic energy of the particle is achieved by submitting the charged particle to the same relatively small potential difference a large number of times, each cycle adding a small amount of energy to the kinetic energy of the particle [3].

This cyclic process of acceleration provides an increase in the electron energy. This is then made to imping on a tangsten target for the production of high energy X-rays, typically for tumour treatment. Moreover, the critical performance optimisation of particle accelerators of any kind depends on particle energy beam position monitoring. For the linear accelerator to be applied successfully in radiotherapy, particularly for intensity modulated and image guided radiotherapy processes, the delivery of the dose to encompass the target volume must be done with great accuracy. The divergence of the beam from the desired position within the waveguide and at the point of striking the tangsten target will diminsh the dose profile of the particle beam. This may result in missing the target volume, leading to an unwanted dose to the healthy tissues and structures surrounding the target volume. To overcome this problem, correct positioning of the beam within the linac waveguide is critical for successful radiotherapy outcomes.

The rest of the paper is organized as follows: within the Introduction, Subsection B introduces some of the relevant background, including information on energy beams for radiotherapy dose optimization. Sub section C discusses BPM in linear accelerators and Sub section D contains information on the use of the transducer for Beam position monitoring. Section II also comprises sub sections A, B, C, D and E in which A introduces the methodology adopted, with specific discussions on simple principles of electromagnetic based simulation of the model. B explains meshing and solver setting for BPM model and C discusses computational experiments made by applying a current carrying wire for Beam Position Monitoring model and E explains the probability density function and the cumulative distribution function applied for BPM. Section III concerns the results and analysis including the principles applied for the determination of cumulative density function for the BPM model and final section concludes the paper.

B. Energy beams for radiotherapy dose optimization

Considerable effort has been expended to analyse the components of linear accelerators for the assessment of beam quality for high precision intensity modulated radiotherapy (IMRT) dose optimisation [4] and for image guided radiotherapy. These have the aim of enabling the irradiation process to deliver the most effective dose to the target volume while the radiation is as low as reasonably achievable (ALARA) [5] to the tissues and structures surrounding the target volume. Therefore, the process of optimized dose delivery in photon radiotherapy is performed by establishing treatment-planning models according to the knowledge of energy beam parameters such as energy beam spectra and variations in the distribution of photons incident on the surface of the target volume [6].

Various methods, particularly Monte Carlo (MC), have been considered for many years as the successful techniques for modeling the beam energy components of the linear accelerator for improving accuracy of the dose delivery process in radiotherapy to overcome the speed issues in performing this analysis. Approximation and simplifications may be necessary which compromise the advantages of Monte Carlo dose calculations [7]. This has provided a motivation to investigate full-wave electromagnetic simulation for the optimization of the critical components of the linac instead of multiphysics simulators to solve the dosimetric problems in radiotherapy.

C. Beam position monitoring in linear accelerators

The main goal of this paper is to establish a non-invasive transverse beam position monitoring model for linear accelerator electromagnetic simulation instead of applying special particle solutions. Beam Position Monitoring (BPM) systems has critical role for any particle acceleration facilities such as linear and circular accelerators. They are applied to maintain a stable and precise beam position to achieve a high level of beam quality critical for the accelerator performance. For synchrotron accelerators and storage rings, precise and stable beam position becomes necessary during the thousands of revolutions of the beam. The efficiency of the BPMs depends upon its ability to measure small

displacements of the beam, compared to its absolute position resolution. Typically the resolution of a system is much better than the accuracy. In most cases, good resolution is much more important than good accuracy. However, it is often appropriate to know the absolute beam position to a fraction of a millimeter, even though the beam motion needs to be known to a few micrometres [8].

Therefore, it is required to constraint the accelerating bunches of electrons throughout the central axis of the waveguide, particularly in the buncher section otherwise their mutual repulsion will lead the electron beam to diverge. This would ultimately produce losses in the beam current as well as serious damage to waveguide structure [2].

D. Pickup for beam position monitoring

Pickup electrodes have been used in particle accelerators for determining the displacement of the energy beam from the desired position in the waveguide. For achieving information about the energy beam position in electron accelerators, several different approaches are present in the literature. Interceptive techniques such as fluorescent screens, wire grids or wire scanners are useful during accelerator installation but cannot be used during accelerator machine operation as they destroy the characteristics of the beam [9]. Even though the electromagnetic pickups are not 'ideal' instruments, they are essential for the operation of the beam. They are still the simplest, fastest and most precise measurement of the beam centre [10].

In a running linac system, the beam must not be disrupted. However, the technique most commonly used to collect information about the spectral content of bunched particle beams is to couple gently to the electromagnetic field of the beam [11]. To comply with this condition, our model of BPM consists of four symmetrically arranged electrode/pickups spaced at 90 degrees, as shown in Fig. 2. Which is in accordance with the conventional technique of using one or two pairs of electrodes, for the measurement of beam offset (i.e. along horizontal and vertical dimention) from its desired position [8]. The pickup electrodes detect the electromagnetic field generated by the conducting filament and convert it to a voltage signal. In order to mimic the real situation of the operating linear accelerator, the use of a current carrying wire in the model is considered as an analogue to the line charge flowing through the centre of the waveguide. Since the electron beam passing through a BPM induces a charge on the pickup electrode, which uniquely depends on the position of the beam and, due to absence of longitudinal variations, the electron beam appears to be essentially a line of moving charge. Measuring the voltage at the pickups can provide the position of the electron beam [12]. This paper verifies the appropriateness of the approach of using a current carrying wire instead of particle beam for beam position monitoring (BPM).

E. Probability density function in application of cumulative density function for BPM data

For the beam position monitoring system, the disadvantage of the peak detection method is that the signal peak voltage is very sensitive to the shape of the pulse, and very sensitive due to attenuation in the cable and also due to signal dispersion in lengthy cables [8]. This situation could be resolved by applying a probability density approach for cumulative distribution function (CDF) in calculating the variations in the measured signal. The approach used in this paper is a 'maximum likelihood' approach obtained from the 50% CDF level, its calculation process can be explained in the following paragraphs.

The probability density function of a continuous valued random variable X is traditionally defined in terms of its probability density function (PDF), f(x), from which probabilities associated with X can be determined using the equation (2) [13].

$$P(a < X \leq b) = \int_a^b f(x)dx \qquad (2)$$

This means the probability that X has a value in the interval [a; b] is the area above this interval and under the graph of the density function. The method for the probability density function estimation (PDF) employed in this study is continuous probability density functions (PDFs) based on a normal kernel function described in detail in [13] and given in equation (3).

$$f(x) \equiv \frac{d}{dx}F(x) \equiv \lim_{n\to\infty}\left(\frac{F(x+h) - F(x-h)}{2h}\right) \qquad (3)$$

In equation (3), F(x) is the cumulative distribution function (CDF) of the random variable x and h is

the ‘bandwidth’. For a random sample of size n from the density f, X: {x1, x2, … xn}, its empirical cumulative distribution function (ECDF) has this expression

$$F'(x) = \frac{\mathrm{N}\{\mathrm{X} \leq \mathrm{x}\}}{n} \quad (4)$$

In equation (4) N{X ⩽ x} shows the number of elements of value less than or equal to x in X. By substituting this to equation (3) it takes the form

$$f'(x) = \frac{N\{(x-h) < x \leq (x+h)\}}{2\mathrm{nh}} \quad (5)$$

This equation can be expressed as (6)

$$\hat{f}(x) = \frac{1}{nh}\sum_{i=1}^{n} K\left(\frac{x-xi}{h}\right) \quad (6)$$

Where as $K(u) = \begin{cases} -\frac{1}{2}, -1 < u < 1, \\ 0, \ otherwise. \end{cases}$ (7)

The equation (6) is a kernel density estimator having a uniform kernel function K. Note this kernel function is a uniform function for the data elements interval of -1 to 1. The kernel bandwidth, *h*, controls the smoothness of the probability density curve, its explanation is given in [13]. In this study the Gaussian kernel function is chosen to achieve much smother PDF which has the following form

$$\mathrm{K}Gaussian = \begin{cases} (2\pi)^{-\frac{1}{2}} e^{-\frac{u^2}{2}}, -1 < u < 1, \\ 0, otherwise. \end{cases}$$

II. METHODOLOGY

A. Simulations

By using a 3D electromagnetic solver [14], the electron beam position was modelled by creating a perfectly conducting cylinder as a waveguide. A current carrying wire of thickness 2mm was placed in the centre of the modelled waveguide as an electron beam (around 2mm being a typical size for the electron beam). It was initially placed at the center of the cylindrical waveguide and its position was calculated using data from the pick-ups. The waveguide length is 160mm as shown in Fig. 2. The beam termination offset is 150mm for the setup of lumped element ports on both sides of the cavity. The outer radius of the main cavity is 55mm and this is also called the beam line radius or waveguide radius. The pick-up electrodes based on the description given in the CST particle studio [14], were modeled as coaxial systems in which the output voltage was measured. We have taken a difference-over-sum approach used in [8], and the voltage signal processing is not performed in hardware or electronics instead an excel spread sheet was used. The variations in the measured voltage of various positions of the ‘beam’ away from the centre provide the information about its displacement from desired position. The BPM data was noted using a CST commercial solver. The variations in the beam position due to its offsets in the transverse plane and with the shift in beam phase from the central axis of the waveguide were determined by time-domain simulations. The radius of each pickup and of inner conductor of the coaxial system was 5mm and its length was 30mm, simulated as a coaxial line. The electrode height was 5mm and the electrode radius was taken as 9.5mm. These symmetrically arranged electrodes/pickups, as shown in Fig. 2, were connected with four discrete ports with an impedance of 50 Ohm each, were used to detect the electromagnetic field generated by the current carrying wire as a voltage signal.

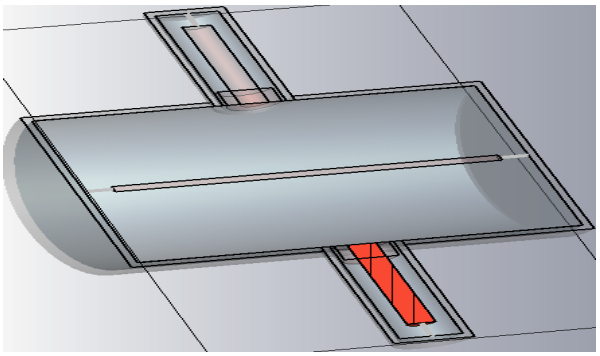

Fig. 2. Cut plane view of the pickup beam position monitoring model.

The behaviour of the electrode was modelled by measuring the voltage signal at the upper port marked as port 3 and the lower port marked as port 4. The beam positional variations are only taken in the transverse direction (i.e along the Y axis) and, for phase analysis, in the XY Plane, which is diagonal to the XY plane in this experiment. For the extraction of the signal from the pickup button, a difference-over-sum scheme was used. One benefit of the difference-over-sum procedure is that it can also be performed in the time domain by using a peak detector to collect the peak voltage in

the bipolar signal from the individual electrodes. The disadvantage of peak detection method is that the peak voltage is very sensitive to the pulse shape and also very sensitive to the measurement system attenuation and dispersion [8]. In order to overcome this situation a probability density approach to cumulative distribution function (CDF) to determine the variation in the measured signal at its 50% level was used, as previously described in subsection E in Section I. The results presented are in good agreement with the trend of data in the published work as shown on page 28 in ref [8], redrawn in Fig. 3.

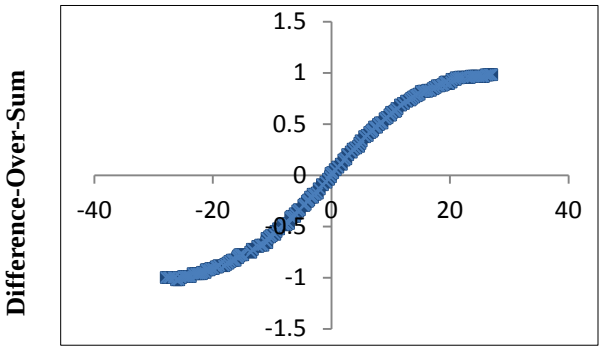

Fig. 3. Beam position monitoring data, redrawn from the reference [8].

B. Meshing and solver parameters settings for the model.

Defining the meshing parameters is an important and critical step for the simulation of any model. For this purpose, hexahedral meshing was used, which is very robust even for most complex imported geometries. The hexahedral mesh in the commercial software [14] used 30 lines per wavelength, a mesh limit of 20 and a meshing line ratio of 15 with a smallest mesh limit of 0.15. After applying this mesh setting, the automatic meshing option provided the following information, the minimum mesh step of 0.4688 and the maximum was 3.38388 and the total mesh cells were 324,131 as sketched in Fig. 4.

The robustness and accuracy of the model was further increased by applying enhance Fast Perfect Boundary Approximation (FPBA). This is because the internally used representation of the model geometries is limited regarding the resolution of the geometrical details if the mesh type "FPBA" is used. The special mesh settings of FPBA have also enhanced FPBA by refining it at PEC/lossy metal edges by a factor of 2. Sub gridding was also used to take the PEC/lossy metal edges into account. The option of density fixing points at the ends of straight lines and for wires was also activated. The choice of fixed points at the elliptical lines or circular edges, and also at fix points for ellipse in case of its diameter larger then 10th of the base mesh points was used. For the background material, the density points, fixing points option was also applied. Also for the advanced meshing, the option of ‘convert geometry data after meshing’ was used for model singularity in case of PEC and lossy metal edges. Due to use of different materials in the model, the material based refinement and consideration of surrounding space for lower mesh limit was also used.

All these above important mesh setting provided the necessary requirements for the model to obtain the optimal results with a reasonable simulation time. The transient solver with an accuracy limit of -30dB was used. The solver settings for ‘source type’ were adjusted for all ports. For the waveguide setting, inhomogeneous port accuracy enhancement (QTM (Quasi-TM) modes) was used and twenty frequency samples were taken. The accuracy of 1% with maximum passes 4 for the line impedance adaptive solver run was implemented.

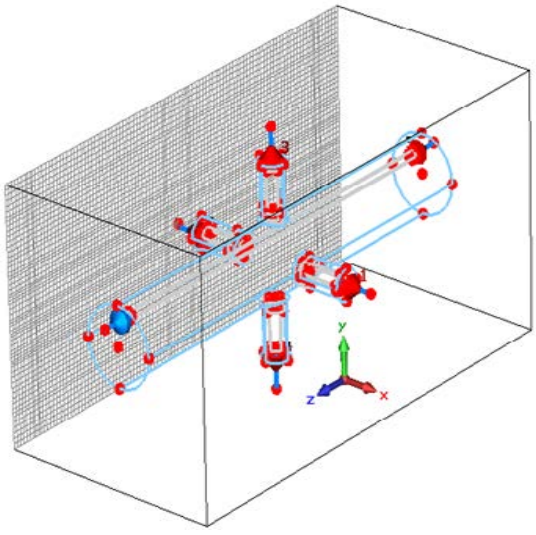

Fig. 4. BPM model with wire frame activated.

The option of absorb unconsidered mode fields for inhomogeneous ports and active Thin Sheet Technology (TST) at ports were applied. The mode calculation frequency during the simulation was 2.856 GHz. In order to meet the steady state criteria, 200 pulses for solver setting were implemented. This parameter needs to be selected with much care since without its optimum selection, the solver will not run. For solver special setting, the stability for time step '1' was chosen.

C. Computational experiments for beam position monitoring

The energy beam, as a current carrying wire, was displaced in the transverse direction to mimic the real situation of beam displacement. The voltage signal from the displaced beam along the various transverse positions was determined at the upper and lower ports. The voltage signal V3 at upper port marked as port 3 and V4 at the lower port marked as port 4 were noted for the tranverse offsets of the beam and the difference over sum of signals from these ports were calculated by using following equation.

$$\frac{\Delta V}{\sum} = \frac{(V3 - V4)}{(V3 + V4)} \qquad (1)$$

The data of voltage signals at the origin and at various offsets with an increment of 1mm up to 24mm was calculated and variations in the voltage signal were determined by computing the difference/sum for each displacement. A kernel density estimator is used to smooth the data and the Cumulative Distribution Function (CDF) is then obtained as in [13]. This is to overcome the drawback of detecting the signal peak method [8]. The CDF values were calculated for different beam offsets in the transverse plane in the +ve and –ve directions. The changes in the voltage signals due to change in the positions of the beam were simulated by determining the variations at 50% of the cumulative density level. 50% was selected simply because of it being a mid-range value and, in general, the turning point for the probability density function: i.e. the peak probability. The results were analysed which showed the values of the voltage signals at 50 % cumulative density function for various displacements of the beam at 2mm with an increment of 1mm up to 24mm from the beam origin.

III RESULTS AND ANALYSIS

A. Beam position monitoring results with cumulative density function

The data obtained by simulation was analysed to obtain voltage signals on the pickup. The energy beam positions simulated at various displacements were determined with respect to the central axis. The CDF curve shown in Fig. 5. is representative of the cumulative distribution function for the beam offset at 11mm from the beam central axis. Similarly, this distribution was calculated for all beam positions by displacing the beam away from the central axis. The CDF data was obtained for beam offsets in the transverse direction i.e on +ve and –ve Y axis and for 45 degrees shift in phase of the beam along the diagonal of the XY plane on the +ve and –ve dimention, the proceeding paragraph and Subsections B, and C further analyse these results.

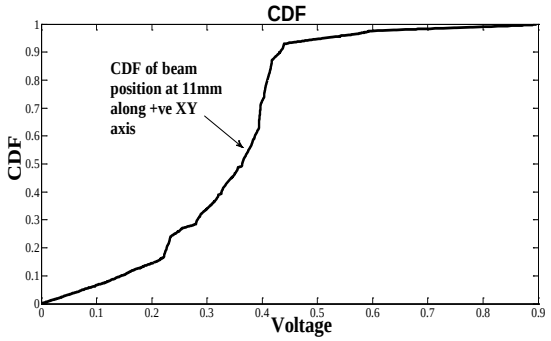

Fig. 5. Data from simulation for cumulated distribution function verses voltage at 11mm beam offset.

The combined graph of 50% CDF values was obtained for all the beam offsets in the range 0 to 24 mm and is presented in the following figures. For illustration purposes, the trend of the CDF plotted values is examined in Fig. 6 by taking only the extremes of maximum and minium beam displacements in the +ve and -ve Y axis. These CDF values of beam offset illustrate the symmetric pattern of the data. To observe the variations in the voltage signals due to a shift in the beam phase of 45 degrees (i.e. on the diagonal of the XY plane), CDF values were calculated in both XY +ve and –ve planes. The trend of the data and their combined symmetric pattern can be observed from Fig. 8. Fig. 7 and 9 represent all the numerical values at the 50% CDF levels for various beam

positions (BP). In Fig. 7, 0 refers to the beam position at the origin and 3mm refers the beam at displacement of 3mm in the transverse plane in +ve Y axis and BP at -3mm referred as beam position at the distance of 3mm in the –ve Y axis. Similarly for the beam position phase analysis in Fig. 9; 0 refers to the beam at the origin, 3 referred beam position at 3mm in the XY plane with the phase angle of 45 degrees and in the –ve XY plane the same position referred as -3mm. The same pattern of beam position representation was used for other beam displacements.

B. Beam position due to transverse offsets

The transverse offsets of the beam positions were determined from the CDF data taken on linear scale. The values of the voltage signals are graphed in Fig. 6 and 7. In Fig. 6, the curve referred to zero voltage is considered as an ideal beam position at the origin. The data was further analysed for the simulated approach to observe any changes that might be present in the linearilty of the data due to the establishment of the current carrying wire approach compared to the particle beam consisting of electron bunches. This has also.validated the approach described in section I. The cumulative

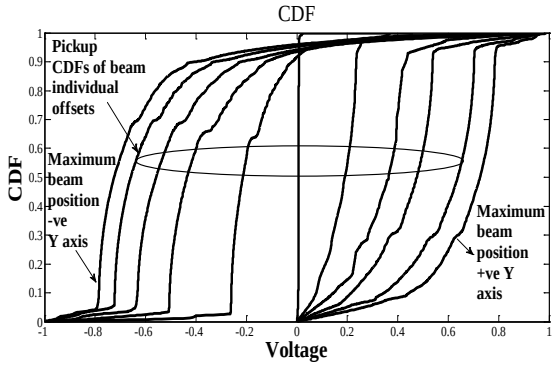

Fig. 6. Combine CDF curves for beam position offsets in transverse plane from beam central axis.

distribution functions (CDF) of the voltage signals were simulated at various displacements with an increment of 1mm, from 2 to 24mm and also in negative directions for same displacements from the central axis. The combined graph of Fig. 6 for various cumulative density functions has shown variations in the voltage signal at 50% of cumulative distribution function (CDF). This means that the signal value changes with respect to beam displacement from its central position considered as the desired beam axis.

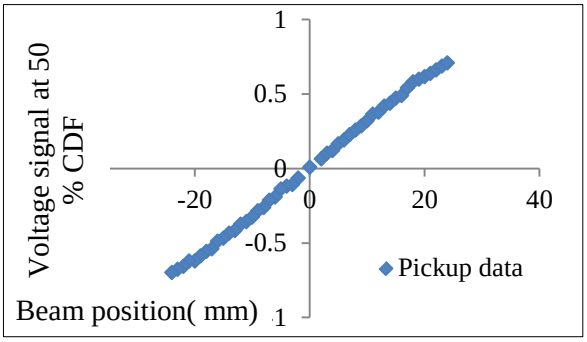

Fig. 7. CDF data for beam position in transverse directions (i.e along +ve and –ve Y axis).

C.Beam phase analysis

The Beam Phase analysis given in Fig. 9 of the combined CDF data shows the computation of the

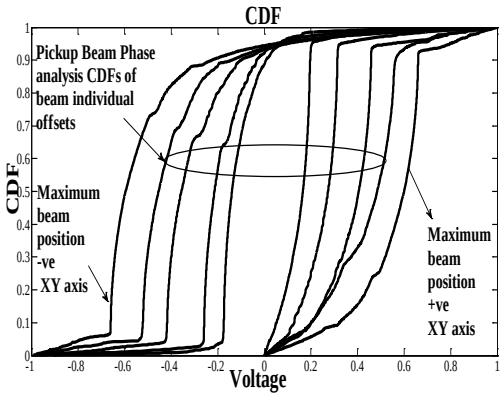

Fig. 8. Combine CDF curves for beam offsets at 45 degrees in XY plane from beam central axis.

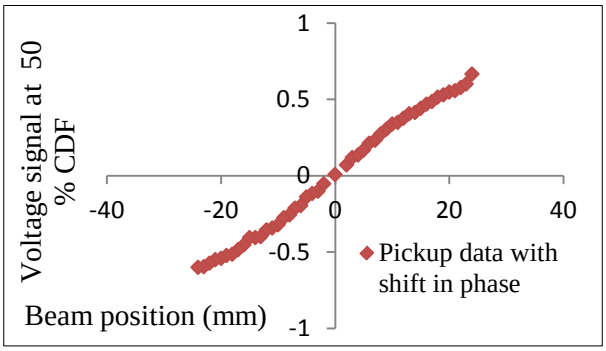

Fig.9. CDF data for beam phase. phase analysis

voltage signal variations for the BPM at 45 degrees with respect to its position at 90 degrees. It shows that a change in the signal appeared as the beam phase angle varies from 90 to 45 degrees with respect to Z axis, it could be observed by comparing the Fig. 7 and 9. The data obtained with change in phase angle of 45 degrees along the +ve and –ve XY plane is drawn in Fig. 9. The graph trend shows that the major effect is due to beam offset in the transverse plane (along Y axis) specially with the shift in the beam phase of 45 degrees (i.e., on the diagonal of the XY plane). A change in the linearity of the graph also appears particularly with the shift of 45 degrees in the beam phase. It has observed that the BPM data obtained from our proposed approach is similar in trend with the data presented in Fig. 3

IV CONCLUSION

A simple and robust model of beam position monitoring (BPM) for the linear accelerator (linac) was obtained using full-wave electromagnetic simulation. A brief review was also presented about electron beam characteristics, beam position monitoring (BPM) concepts and beam parameter processing methods used in particle accelerators. The BPM data was generated through the application of CST 3D electromagnetic software.

The analysis of the data was performed by using a cumulative distribution function (CDF). The cumulative distribution function has provided close approximation to the real situation of the BPM. The simulated results showed the variations in the voltage signal generated at the pickup electrode due to displacement from its central axis and a single numerical value of this voltage signal is obtained from the 50% of the CDF level. The analysis of the model was also made by taking into account the effects of variations in the phase on beam position and its effects on the voltage signal due to displacement of the beam along the horizontal direction. The simulated data of the BPM model was compared with published work, which demonstrates that the behavior of the proposed approach is similar to the data published in [8]. This has validated the approach applied in our study and demonstrates the potential to use a full wave electromagnetics solver to analyse such systems with the result that studies such as probe design and analysis can be undertaken without the need to use Monte Carlo methods and multiphysics/particle simulation software.

REFERENCES

[1] F. M. Khan, *The physics of radiation therapy*. III edition by Lippincott & Wilkins, Q 2003.

[2] L. Loverock, *Linear accelerators*. chapter 11 by Taylor & Francis Group, LLC. 2007.

[3] E. E. B. Podgorsak, *Review of radiation oncology physics: A handbook for teachers and students*, Department of Medical Physics, McGill University Health Centre Montréal, Québec, Canada.

[4] S. Hussain, et al., "Modeling of linear accelerator MLC for the assessment of beam quality dependence in IMRT,'' MSc thesis 2004, School of Physics and Astronomy, The University of Birmingham, Birmingham B15 2TT, UK.

[5] ICRP 26, *Recommendations of the International Commission on Radiological Protection*, Annals of the ICRP 1, 3, 1977.

[6] S. Hussain, "Artificial neural network model for spectral construction of a linear accelerator megavoltage photon beam," UKSim/AMSS IEEE 1st International Conference on Intelligent Systems, Modelling and Simulation, Liverpool, England UK pp. 86–91, 2010.

[7] N. Reynaert, et. al, Monte Carlo treatment planning an introduction, Report 16 of the Netherlands Commission on Radiation Dosimetry,. 2006.

[8] R. E. Shafer, "Beam position monitoring," American Institute of Physics (AIP) conference proceedings, vol. 212, pp. 26 –58, 1989.

[9] C. Peschke, "Higher-Order-Mode Dampfer als Strahllagemonitore,". PhD-thesis, Johann Wolfgang Goethe-Universit_t Frankfurt am Main 2006.

[10] P. Strehl, *Beam instrumentation and diagnostics. Berlin*: Springer-Verlag Berlin Heidelberg, 1st ed., 2006.

[11] I. Podadera, *Tutorial on electromagnetic Beam Position Monitors for Low-β high intensity linacs*, 27 September 2011.

[12] C. D. Chan, "Beam Position Monitor Test Stand," Department of Physics and Astronomy, the Johns Hopkins University, Baltimore, MD, 21218 2004.

[13] J. S. Simonoff, *Smoothing methods in statistics*. New York: Springer Verlag, 1996.

[14] CST, MICROWAVE STUDIO® (CST MWS) and Particle Studio (PS).